Bioactive Materials 5 (2020) 66–73

Contents lists available at ScienceDirect

Bioactive Materials

journal homepage: http://www.keaipublishing.com/biomat

Role of magnesium and aluminum substitution on the structural properties and bioactivity of bioglasses synthesized from biogenic silica

Burcu Karakuzu-Ikizler[a], Pınar Terzioğlu[b], Yeliz Basaran-Elalmis[a], Bilge Sema Tekerek[c], Sevil Yücel[a,*]

[a] Department of Bioengineering, Faculty of Chemistry and Metallurgy, Yildiz Technical University, Istanbul, Turkey
[b] Department of Fiber and Polymer Engineering, Faculty of Engineering and Natural Sciences, Bursa Technical University, Bursa, Turkey
[c] Department of Genetics and Bioengineering, Faculty of Engineering and Architecture, Nişantaşı University, Istanbul, Turkey

ARTICLE INFO

Keywords:
Bioactivity
Biodegradation
Biomaterial
Rice husk silica
SBF

ABSTRACT

The objective of this study was to investigate the effect of magnesium (1 wt%) and aluminum (1 wt%) incorporation on the *in vitro* bioactivity and biodegradation behavior of 45S5 bioactive glasses synthesized from rice husk biogenic silica. The performance of biogenic silica-based samples was compared well with commercial silica-based counterparts. The *in vitro* biodegradation behavior of bioactive glasses was evaluated by the weight loss of samples and pH variation in the Tris buffer solution. Based on composition, bioglasses possessed different properties before and after simulated body fluid (SBF) immersion. The incorporation of magnesium (Mg) and aluminum (Al) enhanced the Vickers hardness of bioglasses. All the bioglasses showed the hydroxyapatite layer formation after SBF treatment as confirmed by the dissolution, FTIR, SEM and XRD analysis, however it was more prominent in the rice husk silica-based 45S5 bioglass. The biogenic silica seems to be a promising starting material for bioglass systems to be used in bone tissue engineering applications.

1. Introduction

Numerous biomaterials are applied for bone regeneration and repair treatments. Bioglass is a widely used hard tissue repair material due to having excellent bioactivity [1]. It can be evaluated in many applications as bone cement, bone grafts, implant coatings, and even in toothpaste [2]. In 1971, the first generation of silicate-based bioglass 45S5 developed with composition of 46.1 mol.% SiO_2–2.5 mol.% P_2O_5–24.4 mol.% Na_2O–26.9 mol.% CaO [3–5]. It has been investigated for about 50 years and is still among the most examined bioactive glass compositions [6].

The successful bioactive glass-living tissue interaction is one of the essential requirements of biomaterial developments [7]. The bioactive glass composition has great importance not only on binding and bone-cell proliferation ability but also on angiogenesis stimulation, anti-inflammatory and anti-bacterial potential during dissolving in the surrounding biological environment [8,9]. Commonly, bioglasses are composed of silica, calcium, phosphate and sodium [6,7]. In recent years, there is a tremendous effort on the addition of trace elements as aluminum (Al), calcium (Ca), cerium (Ce), gallium(Ga), magnesium (Mg), selenium (Se), silver(Ag), strontium (Sr) and zinc (Zn) to the glass systems to further improve the bioactivity, to tailor the degradation rate and to enhance the mechanical strength of the bioglasses [2,9–11]. The incorporation of trace elements may also provide therapeutic functions to bioglasses for regenerative medicine, tissue engineering applications and even bone cancer research [9,11,12].

For instance, it has been shown that the substitution of Mg and Al has considerable influences on the ability of bioactive glasses [13–15]. Magnesium has a stimulatory influence on the development of bone [16]. The incorporation of MgO in the bioactive glass system can provide improved mechanical properties, biocompatibility and biodegradation ability of the glass [17–20]. It was demonstrated that the effect of MgO on hydroxyapatite formation was related to the glass system and MgO content which resulted in enhancement [21,22], reduction [23] or ineffective [24] on hydroxyapatite formation rate. Researchers have reported that aluminum oxide (Al_2O_3) have the property of inhibiting bone-bonding [25], however the addition of aluminum as a part of crystal phase (e.g. aluminosilicate) may overcome this problem [26] as well as maintain an increment in the mechanical properties of glasses [27]. On the other hand, the addition of

Peer review under responsibility of KeAi Communications Co., Ltd.
* Corresponding author. Yildiz Technical University, Faculty of Chemistry and Metallurgy, Bioengineering Department, Esenler, 34210, Istanbul, Turkey.
E-mail addresses: burcukarakuzu@hotmail.com (B. Karakuzu-Ikizler), pinar.terzioglu@btu.edu.tr (P. Terzioğlu), elalmis@yildiz.edu.tr (Y. Basaran-Elalmis), bilgesema.tekerek@nisantasi.edu.tr (B.S. Tekerek), yuce.sevil@gmail.com, syucel@yildiz.edu.tr (S. Yücel).

https://doi.org/10.1016/j.bioactmat.2019.12.007
Received 25 October 2019; Received in revised form 20 December 2019; Accepted 24 December 2019

alumina to the SiO_2–CaO–P_2O_5–K_2O–Al_2O_3 bioglass network might result in an enhancement in the mechanical properties such as compressive strength and elastic modulus of the glass due to the alumina (Al_2O_3/K_2O) concentration [28]. Contrarily, the bioglasses containing Al_2O_3 with high molar concentrations(1.5–2.5%) showed cytotoxic effect against cell lines although the other bioglasses (0–1.0% Al_2O_3) were almost non-toxic [28]. Therefore, the investigations on the effect of magnesium and aluminum addition to the final properties of bioglass systems are an important issue.

Commercial silica precursors as tetraethyl orthosilicate [18,29,30], Belgian quartz sand [31] and silicon dioxide [32] have been mainly used for bioglass synthesis. Recently, Yucel et al. highlighted the use of rice husk ash silica for bioactive glass production [33]. In this pre-study, it was found that the bioactive glass is capable of forming a hydroxyapatite layer after immersion in simulated body fluid (SBF). At present, there is not enough information in the scientific literature for the utilization of biogenic silica as alternative sources to prepare bioglasses. Thus, rice husk ash is an alternative low-cost and abundant silica precursor that can be used during the fabrication of the glasses.

The main objective of this study is to evaluate rice husk ash silica for the production of Al and Mg incorporated melt derived 45S5 bioglasses; in particular, their biodegradation behavior in the Tris solution was compared with counterparts bioglasses which produced by commercial silica. On the other hand, the study presents the effect of substitution of Al and Mg on final properties *in vitro* bioactivity behavior of 45S5 glass systems in terms of Vickers hardness measurements, SEM and XRD techniques.

2. Materials and methods

2.1. Materials

The chemicals used in experiments as Al_2O_3, HCl, NaOH, NaCl, KCl, $MgCl_2.6H_2O$, $MgSO_4.7H_2O$, Na_2SO_4, $Na_2HPO_4.2H_2O$, $NaHCO_3$, $(CH_2OH)_3CNH_2$ and $CaCO_3$, $CaCl_2.2H_2O$ were supplied by Merck (Darmstadt, Germany). SiO_2 was supplied by Riedel-de Haën. The rice husk ash (Yetiş Food Factory, Turkey) was used as a raw material for silica extraction.

2.2. Preparation of biogenic silica powder

As a first step, the rice husk ash submitted to heat treatment in a porcelain crucible in a muffle furnace (600 °C, 5 h). Followed by the removal of cationic impurities using acid leaching pretreatment. Acid leached rice husk ash was prepared by mixing 40 g of the sample with 240 mL of distilled water and an appropriate quantity of hydrochloric acid solution (pH = 1). Subsequently, the mixture was refluxed with constant stirring. After 2 h, the dispersion was filtered and the upper carbon residues were dried in an oven (80 °C, 20 min). After drying, the ashes were mixed with 1 M NaOH solution (240 mL) for 60 min under continuous stirring (750 rpm) at 100 °C. The sodium silicate solution was obtained by filtration the dispersion and washing thoroughly the remnants of carbon with distilled water (400 mL). The solution was cooled down to 25 °C. Finally, the silica gel was prepared by adjusting the pH of the solution with diluted hydrochloric acid solution to a constant pH (pH = 9) with constant stirring. The one-day aged silica gels were crushed and then centrifuged for 15 min at 2500 rpm. The supernatant solution was poured, and the gels were washed with distilled water by repeating four times. The final product was obtained by drying the powders in an oven (80 °C, 12 h) [34]. Silica particles were ground by mortar two-fold to obtain final biosilica.

2.3. Synthesis of melt-derived bioactive glasses

The compositions of bioglasses synthesized through the melting process are given in Table 1 [35]. The $CaCO_3$, $Na_2HPO_4.2H_2O$, $NaHCO_3$, $MgSO_4.7H_2O$, Al_2O_3 and SiO_2 or biogenic silica were ground twice to provide homogeneity. The bioglasses were prepared as described by Karakuzu-İkizler et al. [10].

Table 1
The chemical composition of bioglasses.

Sample	Bioglass Chemical Composition (wt.%)					
	SiO_2	Na_2O	CaO	P_2O_5	MgO	Al_2O_3
S5	45	24.5	24.5	6	–	–
S5Mg[a]	45	24.5	23.5	6	1	–
S5MgAl[a]	45	23.5	23.5	6	1	1

[a] Rice or commercial added near the symbolic names when biogenic and commercial silica was used, respectively.

2.4. In vitro bioactivity studies

The formation of hydroxyl carbonate apatite (HCA) on the bioglass surfaces was examined after immersion in SBF (pH = 7.4) at 37 °C up to 28 days. The SBF was prepared with an ion concentration of Na^+ 142.0, K^+ 5.0, Ca^{2+} 2.5, Mg^{2+} 1.5, Cl^- 125.0, HPO_4^{-2} 1.0, HCO_3^- 27.0, SO_4^{-2} 0.5 mmol/L in the distilled water [10,15].

2.5. Biodegradation studies

The *in vitro* degradation assessment was accomplished through immersing bioglasses in tris-(hydroxymethyl)-aminomethane (Tris) buffer solution up to 7 days at 37 °C. The pH variation measurement of the Tris solution and sample weight changes were collected to determine degradation behavior.

2.6. Characterization studies

The morphologies of the bioglasses were determined using JSM-5410LV Scanning Microscope (Japan). The change in the ion concentration (aluminum, calcium, magnesium phosphorus, silica, and sodium) of SBF was monitored using an Inductively Coupled Plasma Optical Emission Spectrometer (PerkinElmer Optima 2100 DV, USA). The composition of phase and surface crystallization of the bioglasses were examined using X-ray Diffraction instrument (X'pert Pro Pan'alytical) run at 40 kV and 45 mA with an angular range 2θ = 5° - 90° and a step size of 0.03°. FT-IR study of the bioglasses were performed on a SHIMADZU, IR Prestige 21; USA, in the range of 600–4000 cm^{-1} during 64 scans, with 4 cm^{-1} resolution before and after immersion in SBF. The mechanical properties of the bioglasses were determined using a Vickers hardness instrument (Bulut Makina HVS 1000, Turkey). The Vickers indentations were collected within 5 s using 500 gf of loading. The results of triplicate measurements were expressed as mean ± standard deviation. The significance between means was analyzed by ANOVA procedures by using SPSS software program, p values < 0.05 were regarded as significant.

3. Results and discussion

3.1. Vickers hardness of bioglasses

The Vickers Hardness presents very beneficial information regarding the surface structural behavior of the bioglasses [36]. The changing trend in the mechanical properties of glasses was examined after immersion in SBF up to 21 days. The Vickers microhardness of the bioglasses are shown in Table 2. Cannillo et al. and Goller et al. reported a 474.1 (46.4) and 383 (60) microhardness value for their 45S5 bioglasses, respectively [37,38]. The microhardness values of biosilica based 45S5 bioglasses obtained in this study were relatively higher than the values reported in the literature. It was observed that the

Table 2
Vickers hardness (HV) values for bioglasses prior to and later immersion in SBF.

Samples	HV (kg/mm^2)				HV reduction (%)		
	Before SBF	7. Day SBF	14. Day SBF	21. Day SBF	7. Day	14. Day	21. Day
S5 rice	523 ± 11.0	191 ± 6.5	135 ± 6.0	98 ± 5.5	61	72	79
S5 commercial	405 ± 9.0	179 ± 7.1	144 ± 5.5	104 ± 4.5	56	64	74
S5Mg rice	434 ± 12.0	133 ± 5.0	122 ± 6.0	101 ± 5.2	71	72	77
S5Mg commercial	400 ± 10.0	156 ± 7.5	132 ± 5.5	113 ± 3.3	61	67	71
S5MgAl rice	559 ± 11.0	196 ± 6.0	153 ± 6.5	141 ± 3.5	65	73	75
S5MgAl commercial	511 ± 10.0	195 ± 6.5	150 ± 7.5	132 ± 5.2	62	71	74

substitution of a part of calcium and sodium ions with both magnesium and aluminum ions enhanced the mechanical properties. S5MgAl rice sample had the highest hardness. The Vickers hardness measurements exhibited that the hardness values decreased with the increment of immersion time. It can be explained by the dissolution of calcium and sodium ions from bioglass. Subsequent to the interaction of these ions with phosphate ions available in SBF, the HCA precipitation forms on the surface of the bioglasses.

After immersion in SBF for 7 days, Mg incorporated bioglass showed the highest reduction between samples produced from rice husk ash silica. As can be seen from Table 2, the variation of Vickers hardness of Al_2O_3 incorporated bioglass was smaller compared to other samples' hardness values after immersion in the SBF solution for 7 days. However, the reduction of Vickers hardness of Al_2O_3 incorporated bioglasses was closer to all the other samples' values at 21 days of immersion in the SBF solution. The variation of Vickers hardness of all the samples produced by the use of rice husk silica was close to each other after immersion in the SBF solution for 21 days.

3.2. SEM analysis of bioglasses

Micrographs of all bioglasses prior to and later immersion in SBF solution at different time periods were screened to observe the microstructural evaluation of samples. Fig. 1 and Fig. 2 show the micrographs of bioglasses. According to the SEM micrographs (Fig.s 1-a, 1-e, 1-i, 2-a, 2-e, 2-i), the surface of bioglasses was smooth and glassy before immersion in SBF solution. After 7 days, all the bioglasses were covered by apatite-like crystals with variable shape and size at their surfaces (Fig.s 1-b, 1-f, 1-k and 2-b, 2-f, 2-k) as reported earlier for various bioglass systems [10,39–41]. The formation of spherical hydroxyapatite structures was more on the S5 rice, S5MgAl rice and S5Mg commercial samples surface as against surfaces of other bioglasses. Generally, apatite crystals precipitation starts via the occurrence of sole granules followed by the formation of a dense layer on the bioglass surface due to the granules' progressive grow [33]. At the same time, the creation of cracks which is also the proof of biodegradation can be explained by the quick release of ions from bioglass after immersion in the SBF solution. The release of cations leads to the development of the tensile strain on the surface of the bioglasses and followed by crack formation [40]. The HCA layer formation raised steadily and homogenously with the increase of immersion time from 14 to 21 days, especially in the commercial silica-based ones.

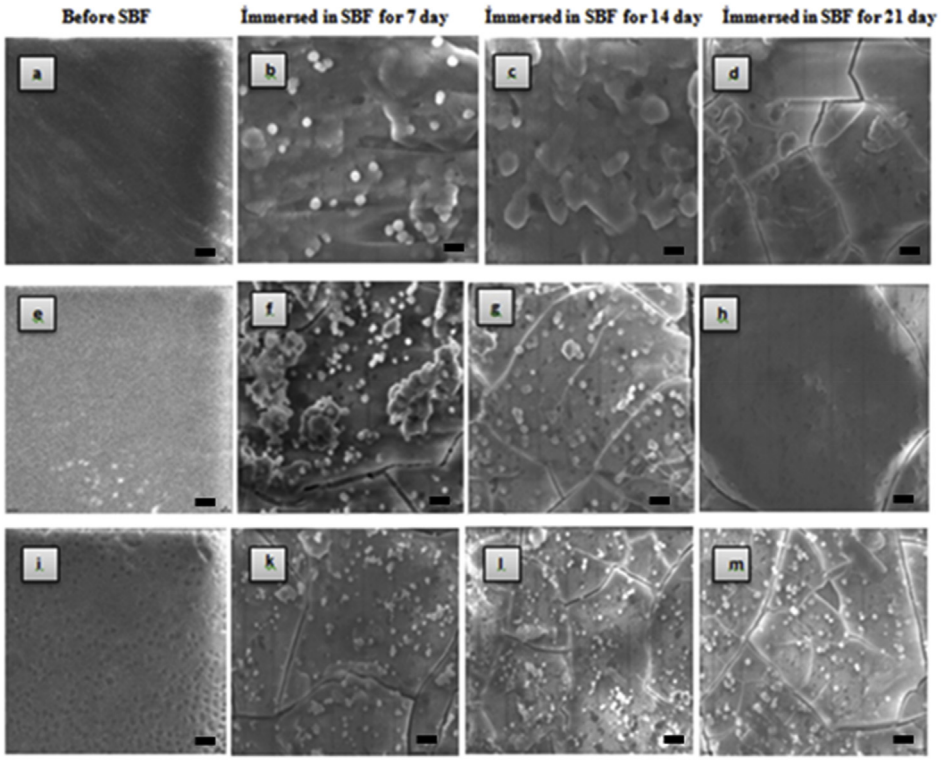

Fig. 1. SEM micrographs of rice husk ash silica-based glass samples surface (a–d) S5 rice (e–h) S5Mg rice (i–m) S5MgAl rice. Magnification: × 1000; Scale bar: 10 μm.

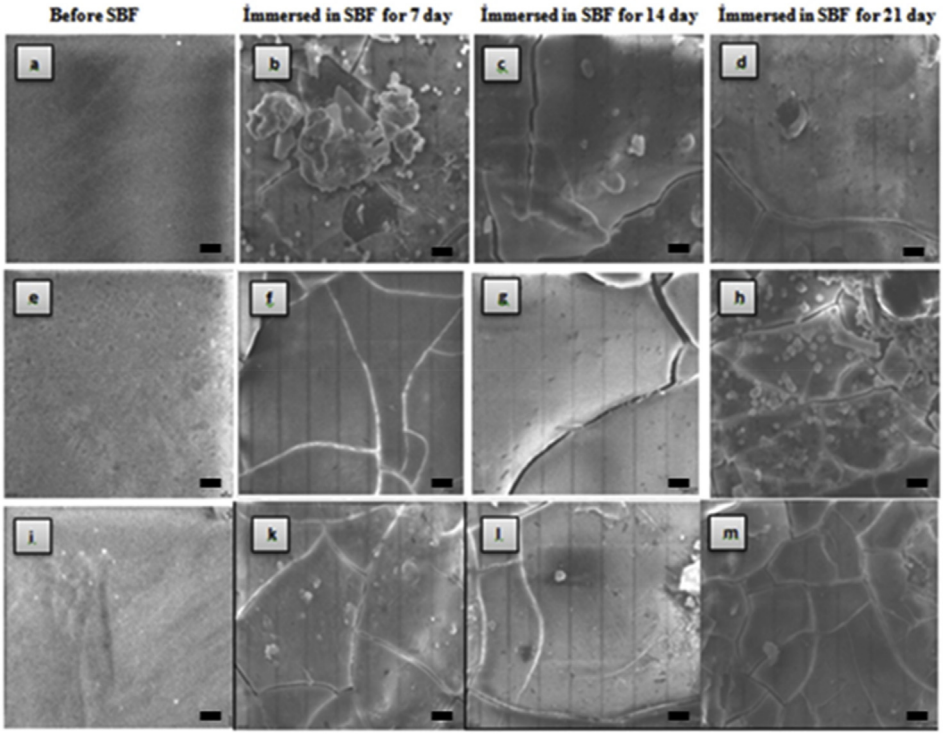

Fig. 2. SEM micrographs of commercial silica-based glass samples surface (a–d) S5 commercial (e–h) S5Mg commercial (i–m) S5MgAl commercial. (Magnification: × 1000; Scale bar: 10 μm)

3.3. XRD analysis of bioglasses

Apatite formation on the bioglass surface was expected after SBF immersion. In order to confirm the apatite formation, prepared bioglass samples were subjected to XRD analysis before and after the SBF immersion. The XRD patterns are presented in Fig. 3. XRD pattern of the S5 rice sample before SBF immersion (Fig. 3a) shows no crystalline diffraction peaks. A similar XRD pattern was obtained by Mozafari et al. [42]. for a sol-gel derived bioglass before SBF immersion and it was attributed to the glassy nature of the material. In a study conducted by Boccaccini et al. [43]. melt derived glasses were produced in a similar method used in this study, and a similar XRD pattern (without crystalline diffraction peaks) was obtained. This XRD pattern was stated as a proof of the amorphous Bioglass® structure [43]. Thus, S5 rice glass sample was identified to be amorphous when the results of literature and obtained XRD patterns were compared. As can be seen in Fig. 3b–d after SBF immersion obvious crystalline phases were formed on the surfaces of the glass samples. These formations were identified as crystalline hydroxyapatite (card#01-074-0565).

The XRD patterns of S5 rice and S5 commercial sample after immersion in the SBF solution for 28 days showed that both samples had apatite-like layer peaks nearly at the same 2θ degrees which approved rice husk ash silica-based sample's bioactivity was very similar to the commercial silica-based sample. As can be seen from Fig. 3-d, the incorporation of MgO and Al_2O_3 to commercial silica-based samples did not have a negative effect on apatite-like layer formation on glass surfaces.

3.4. Change of ion concentrations in SBF solution

The observation of apatite formation ability by immersing ceramics in simulated body fluid is one of the widely used methods since 1987 [44]. The variations of Si^{4+}, P^{5+} and Ca^{2+}concentrations after rice husk silica-based bioglasses immersed in the SBF solution at 28 days are given in Fig. 4.

The Si concentrations in the SBF solution for all bioglasses were considerably increased. Similar results were obtained for silica-based glasses in the literature [10,45]. As can be observed in all cases, Ca^{2+} ions ions released from the structure of bioglasses and present in SBF solution were complitely transfered to the bioglass surface, most probably to form the hydroxyapatite layer.. The contact of bioglass with SBF solution was monitored and deficiency of Ca^{2+} concentration in the SBF solution was observed. Reddy and Kiran explained this situation that the dissolved Ca^{2+} ion leads to the formation of silanol groups (Si–OH) followed by silica gel layer occurrence on to the sample surface. PO_4^{3-} ion together with Ca^{2+} ion was involved in the structure of calcium phosphate and then hydroxy carbonate apatite formed [46]. The ion concentration of P^{5+} in the SBF solution was about the same in all cases. Only the S5 rice immersed SBF solutions' Si^{4+} concentration was the -most which is may be indicating the hydroxyl carbonate apatite growth was probably more on the S5 rice sample, since it is indicating the higher dissolution behavior of this glass sample.

3.5. FT-IR analysis of bioactive glasses

Detailed information regarding intermolecular interactions of bioactive glass samples before and after immersion in SBF solution from the FT-IR spectrums are given in Table 3. FTIR spectra of different bioglasses obtained in this study showed small changes in intensity and wavenumbers.

The noticed peaks in the spectrum of S5 rice sample prior to SBF were as follows (i) at 706 cm^{-1} and 858 cm^{-1}/the Si–O–Si stretching vibrations, (ii) at 981 cm^{-1}/a phosphate group (PO_4^{3-}), (iii) at 1650 cm^{-1}, 3000 cm^{-1} - 3700 cm^{-1}/H – OH bending vibrations [47].

The FT-IR spectrum of S5 rice sample after immersion in SBF indicates the presence of the P–O bending vibrations in hydroxyapatite crystalline lattice due to the bands between 950 cm^{-1} and 1040 cm^{-1}. Additionally, the absorption bands at 1411 cm^{-1} and 1458 cm^{-1} was assigned to carbonate group (CO_3^{2-}) that were evidence of hydroxyapatite layer formation on the surface of samples [48].The peaks at

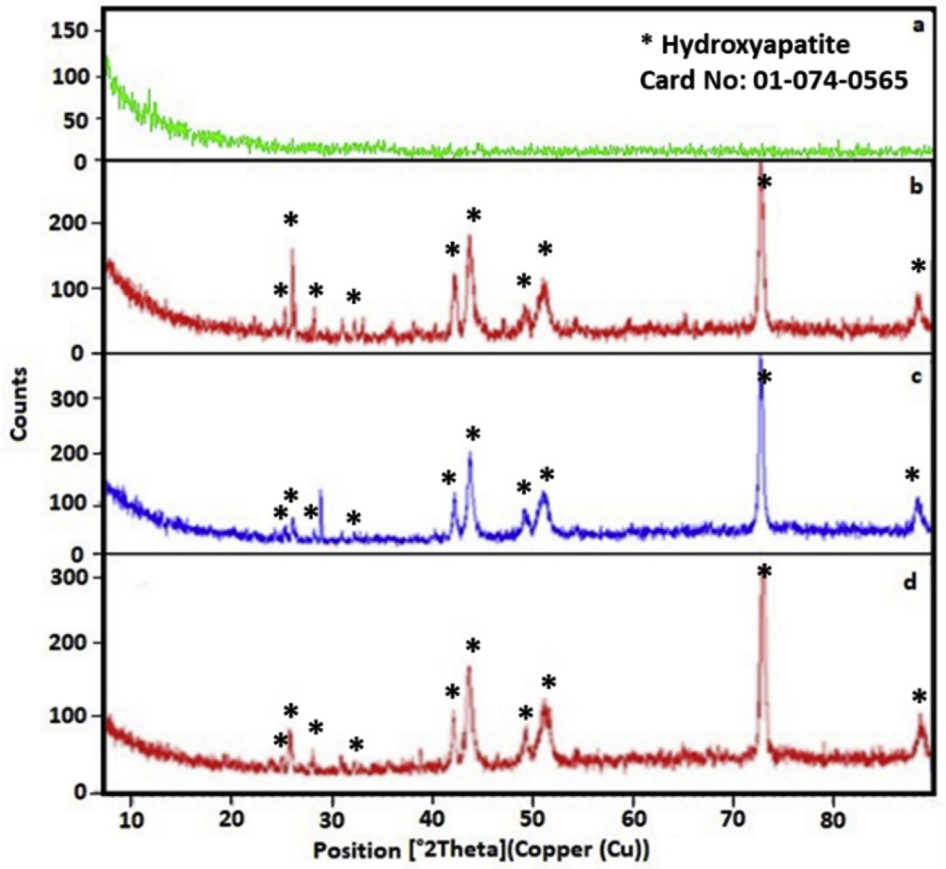

Fig. 3. XRD patterns of a) S5 rice sample before immersion; bioglasses at 28 days of immersion in SBF b) S5 rice c) S5 commercial d) S5MgAl commercial sample.

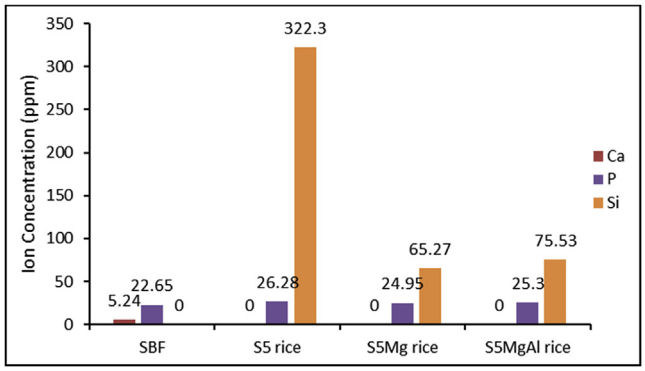

Fig. 4. The changes in SBF solution by immersion of rice husk ash silica-based bioactive bioglasses at 28 day.

1639 cm^{-1} and between 3000 cm^{-1} - 3700 cm^{-1} were related to the H – OH bending vibrations of the water molecules.

When the FT-IR results of the -undoped, Mg and both Mg and Al doped rice husk silica-based samples after immersion in SBF were compared, there were variation in their intensities for the peak at around 1050 cm^{-1} which was related to the precipitated calcium phosphate groups. The intensity of the peak was in the following order: S5 rice sample > S5MgAl rice > S5Mg rice. Furthermore, the intensity of peaks at 1411 cm^{-1} and 1458 cm^{-1} due to C–O stretching in carbonate groups (CO_3^{2-}) were highest for S5 rice bioglass [48]. The FT-IR results indicated that the S5 rice sample had the highest bioactivity which was also supported by XRD and ICP analyses results.

According to FT-IR results, the highest intensity that belongs to calcium phosphate peak (1050 cm^{-1}) was observed for MgO incorporated commercial silica based bioglass indicating that MgO incorporation increased the bioactivity of glasses as distinct from rice hull ash silica-based samples.

3.6. Biodegradation behavior of glasses

The contact of bioactive glasses with Tris solution causes Ca, Na, P, and Si ions release from bioglass to the environment. The bioglass loses weight due to ion transfer. The weight loss of bioglass presents information on the bioactivity behavior of glass. The *in vitro* dissolution behaviors of produced bioglasses were analyzed by the weighting of glasses and the pH change of the Tris solution. Fig. 5 shows the dissolution of bioglasses in Tris solution during 7 days of immersion. The Tris buffer solution has no free ions, and thus ion dissolution can be observed clearly with weight loss and pH value variation in this buffer solution. The weight of bioactive glasses decreased by the increase of time due to the ion dissolution rates. Weight loss changes of S5MgAl and S5Mg rice samples were slightly higher. After two days, the weight of glass samples decreased continuously at a slow rate. It can be seen from Fig. 5 that after 4 days, dissolution rates were slower than the first 3 days. It can be explained by the fact that the weight of bioglasses increased due to precipitation of released ions as hydroxyapatite on glass surface from Tris solution. The dissolution behavior of rice husk ash silica and commercial silica-based bioglasses were similar to each other.

Fig. 6 shows the change in pH values of Tris solution after the immersion of rice husk ash silica and commercial silica-based glass samples. . As previously shown in the literature, the contact of glass samples caused an increase in Tris solution pH which was in accordance with the release of ions from the surface of bioglass which directs to attack silica network and followed by silanol formation [40,50].

Table 3
Assignment of FT-IR bands for bioglasses prior to and later immersion in SBF.

Wave numbers (cm^{-1})				Comparison of peaks of S5Mg and S5MgAl with S5 rice	Assigned Structural Units
S5 rice prior to immersion	S5 rice later immersion	S5Mg and S5MgAl rice later immersion	S5Mg and S5MgAl commercial later immersion		
3700–3000	3700–3000	3700–3000	3700–3000	Smaller intensity	H–OH bending vibrations [47]
1650	1650	1639	1639	Smaller intensity Shift to smaller wavenumber	H–OH bending vibrations [47]
1405	1411 and 1458	1411 and 1458	1411 and 1458	–	C–O stretching in carbonate groups [10,48]
1050	1040	1000	1000	Shift to smaller wavenumber	Asymmetric Si–O–Si and ionic character of PO_4^{-3} vibrations [16,49]
858	858	858	858	Smaller intensity	Si–O–Si stretching and acidic phosphate group vibrations [16,49]
798	798	798	798	798	Repolymerization of Si–O–Si [16,49]
706	706	706	706	706	Si–O–Si stretching vibrations [10]

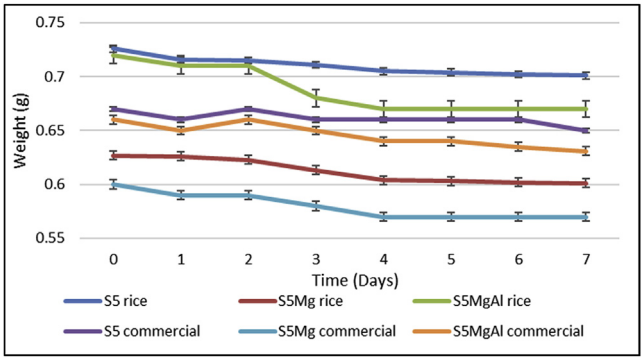

Fig. 5. Representative images showing the weight loss of bioglasses in Tris solution.

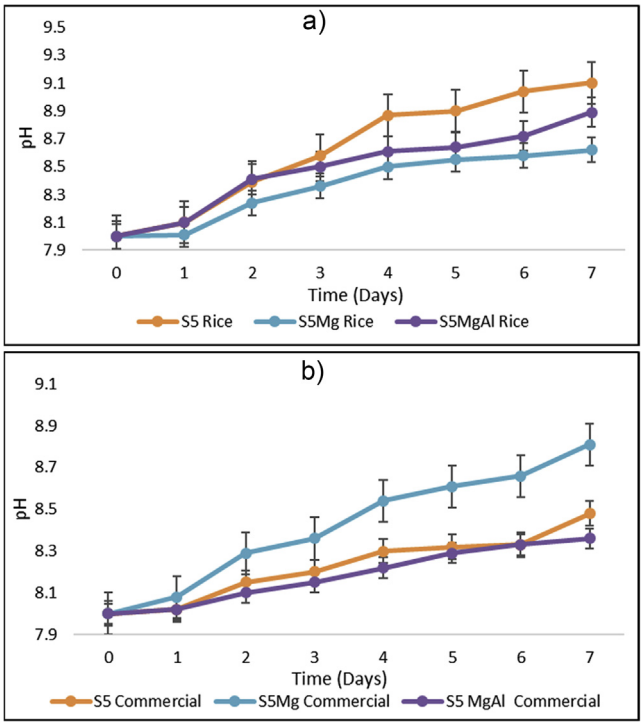

Fig. 6. Representative images showing the pH variation of Tris solution with immersion time periods.

The Tris solution pH increment from the highest to the lowest was obtained with the immersion of S5 rice, S5MgAl rice, and S5Mg rice bioglass, respectively. The higher pH changes in S5 rice sample immersed in the Tris solution demonstrated that S5 rice sample had higher reactivity than the other rice husk ash silica-based samples. The higher pH change was observed for the S5Mg commercial sample. It is remarkable that the MgO substitution has a favorable influence on the bioactivity of the commercial silica-based sample. This result has verify the results of XRD analysis (data not shown) which are well-nigh to the published data [18]. As can be seen from Fig. 6-b, the pH change was clearly greatest in S5 rice immersed in the Tris solution, thus approving S5 rice sample had a higher bioactivity than the S5 commercial sample.

4. Conclusion

In conclusion, low-cost biosilica source - rice husk ash-has been successfully applied to synthesize magnesium and aluminum incorporated 45S5 bioactive glasses by the melting technique. Addition of aluminum and magnesium have not shown any negative influence on the bioactivity and biodegradability of the rice husk ash silica-based

glass samples as confirmed by results of SEM, XRD and *in vitro* studies. However, the addition of aluminum together with magnesium enhanced the hardness of biogenic and commercial silica-based bioglasses. Moreover, magnesium incorporation enhanced the bioactivity and biodegradability of the commercial silica-based glass samples. The results showed that the type of silica and substitution element have a significant role in the final properties of bioglasses.

Declaration of competing interest

The authors declares that they have no conflict of interest.

Acknowledgments

This work was supported by Research Fund of the Yildiz Technical University [Project Number: 2013-07-04-KAP06].

References

[1] X. Wang, J. Ye, Y. Wang, L. Chen, Self-setting properties of a β-dicalcium silicate reinforced calcium phosphate cement, J. Biomed. Mater. Res. B Appl. Biomater. 82 (2007) 93–99, https://doi.org/10.1002/jbm.b.30709.

[2] H. Tripathi, C. Rath, A.S. Kumar, P.P. Manna, S.P. Singh, Structural, physico-mechanical and *in-vitro* bioactivity studies on SiO_2–CaO–P_2O_5–SrO–Al_2O_3 bioactive glasses, Mater. Sci. Eng. C 94 (2019) 279–290, https://doi.org/10.1016/j.msec.2018.09.041.

[3] Y.C. Fredholm, N. Karpukhina, R.V. Law, R.G. Hill, Strontium containing bioactive glasses: glass structure and physical properties, J. Non-Cryst. Solids (2010) 2546–2551, https://doi.org/10.1016/j.jnoncrysol.2010.06.078.

[4] L.L. Hench, R.J. Splinter, W.C. Allen, T.K. Greenlee, Bonding mechanisms at the interface of ceramic prosthetic materials, J. Biomed. Mater. Res. 5 (1971) 117–141, https://doi.org/10.1002/jbm.820050611.

[5] P. Sepulveda, J.R. Jones, L.L. Hench, Characterization of melt-derived 45S5 and sol-gel-derived 58S bioactive glasses, J. Biomed. Mater. Res. 58 (2001) 734–740, https://doi.org/10.1002/jbm.10026.

[6] L.L. Hench, J.K. West, Biological applications of bioactive glasses, Life Chem. Rep. 13 (1996) 187–241 Open Access Libr http://www.oalib.com/references/7463840.

[7] L.L. Hench, I. Thompson, Twenty-first century challenges for biomaterials, J. R. Soc. Interface 7 (Suppl 4) (2010) S379–S391, https://doi.org/10.1098/rsif.2010.0151.focus.

[8] A. Hoppe, N.S. Güldal, A.R. Boccaccini, A review of the biological response to ionic dissolution products from bioactive glasses and glass-ceramics, Biomaterials 32 (2011) 2757–2774, https://doi.org/10.1016/j.biomaterials.2011.01.004.

[9] S. Kargozar, F. Baino, S. Hamzehlou, R.G. Hill, M. Mozafari, Bioactive glasses entering the mainstream, Drug Discov. Today 23 (2018) 1700–1704, https://doi.org/10.1016/j.drudis.2018.05.027.

[10] B. Karakuzu-İkizler, P. Terzioğlu, B.S. Oduncu-Tekerek, S. Yücel, Effect of selenium incorporation on the structure and *in vitro* bioactivity of 45S5 bioglass, J. Australas. Ceram. Soc. (2019), https://doi.org/10.1007/s41779-019-00388-6.

[11] A.M. Deliormanlı, Synthesis and characterization of cerium- and gallium-containing borate bioactive glass scaffolds for bone tissue engineering, J. Mater. Sci. Mater. Med. 26 (2015) 1–13, https://doi.org/10.1007/s10856-014-5368-0.

[12] K.S. Rana, L.P. de Souza, M.A. Isaacs, F.N.S. Raja, A.P. Morrell, R.A. Martin, Development and characterization of gallium-doped bioactive glasses for potential bone cancer applications, ACS Biomater. Sci. Eng. 3 (2017) 3425–3432, https://doi.org/10.1021/acsbiomaterials.7b00283.

[13] C. Ohtsuki, T. Kokubo, T. Yamauro, Compositional dependence of bioactivity of glasses in the system CaO-SiO_2-Al_2O_3: its *in vitro* evaluation, J. Mater. Sci. Mater. Med. 3 (1992) 119–125, https://doi.org/10.1007/BF00705279.

[14] K. Ohura, T. Nakamura, T. Yamamuro, Y. Ebisawa, T. Kokubo, Y. Kotoura, M. Oka, Bioactivity of CaO·SiO_2 glasses added with various ions, J. Mater. Sci. Mater. Med. 3 (1992) 95–100, https://doi.org/10.1007/BF00705275.

[15] A. Goel, R.R. Rajagopal, J.M.F. Ferreira, Influence of strontium on structure, sintering and biodegradation behaviour of CaO-MgO-SrO-SiO_2-P_2O_5-CaF_2 glasses, Acta Biomater. 7 (2011) 4071–4080, https://doi.org/10.1016/j.actbio.2011.06.047.

[16] K. Kaur, K.J. Singh, V. Anand, G. Bhatia, S. Singh, H. Kaur, D.S. Arora, Magnesium and silver doped CaO–Na_2 O–SiO_2 –P_2O_5 bioceramic nanoparticles as implant materials, Ceram. Int. 42 (2016) 12651–12662, https://doi.org/10.1016/j.ceramint.2016.05.001.

[17] C. Knabe, M. Stiller, G. Berger, D. Reif, R. Gildenhaar, C.R. Howlett, H. Zreiqat, The effect of bioactive glass ceramics on the expression of bone-related genes and proteins *in vitro*, Clin. Oral Implant. Res. 16 (2005) 119–127, https://doi.org/10.1111/j.1600-0501.2004.01066.x.

[18] A. Saboori, M. Rabiee, F. Moztarzadeh, M. Sheikhi, M. Tahriri, M. Karimi, Synthesis, characterization and *in vitro* bioactivity of sol-gel-derived SiO_2-CaO-P_2O_5-MgO bioglass, Mater. Sci. Eng. C 29 (2009) 335–340, https://doi.org/10.1016/j.msec.2008.07.004.

[19] J. Soulié, J.M. Nedelec, E. Jallot, Influence of Mg doping on the early steps of physico-chemical reactivity of sol–gel derived bioactive glasses in biological medium, Phys. Chem. Chem. Phys. 11 (2009) 10473, https://doi.org/10.1039/b913771h.

[20] X. Chen, X. Liao, Z. Huang, P. You, C. Chen, Y. Kang, G. Yin, Synthesis and characterization of novel multiphase bioactive glass-ceramics in the CaO-MgO-SiO_2 system, J. Biomed. Mater. Res. B Appl. Biomater. 93 (2010) 194–202, https://doi.org/10.1002/jbm.b.31574.

[21] A. Moghanian, A. Sedghi, A. Ghorbanoghli, E. Salari, The effect of magnesium content on *in vitro* bioactivity, biological behavior and antibacterial activity of sol–gel derived 58S bioactive glass, Ceram. Int. 44 (2018) 9422–9432, https://doi.org/10.1016/j.ceramint.2018.02.159.

[22] M. Erol, A. Özyuguran, Ö. Çelebican, Synthesis, Characterization, and *in vitro* bioactivity of sol-gel-derived Zn, Mg, and Zn-Mg Co-doped bioactive glasses, Chem. Eng. Technol. 33 (2010) 1066–1074, https://doi.org/10.1002/ceat.200900495.

[23] J. Ma, C.Z. Chen, D.G. Wang, Y. Jiao, J.Z. Shi, Effect of magnesia on the degradability and bioactivity of sol-gel derived SiO_2-CaO-MgO-P_2O_5 system glasses, Colloids Surfaces B Biointerfaces 81 (2010) 87–95, https://doi.org/10.1016/j.colsurfb.2010.06.022.

[24] J.S. Moya, A.P. Tomsia, A. Pazo, C. Santos, F. Guitián, *In vitro* formation of hydroxylapatite layer in a MgO-containing glass, J. Mater. Sci. Mater. Med. 5 (1994) 529–532, https://doi.org/10.1007/BF00124885.

[25] L.L. Hench, Bioceramics: from concept to clinic, J. Am. Ceram. Soc. 74 (1991) 1487–1510, https://doi.org/10.1111/j.1151-2916.1991.tb07132.x.

[26] Y. Liu, X. Sheng, X. Dan, Q. Xiang, Preparation of mica/apatite glass-ceramics biomaterials, Mater. Sci. Eng. C 26 (2006) 1390–1394, https://doi.org/10.1016/j.msec.2005.08.017.

[27] F.M. Stábile, C. Volzone, J. Ortiga, Thermal evolution of Na_2O-K_2O-CaO-SiO_2-P_2O_5-Al_2O_3 glass system, and possible applications as biomedical devices, Procedia Mater. Sci. 8 (2015) 332–337, https://doi.org/10.1016/j.mspro.2015.04.081.

[28] H. Tripathi, S. Kumar Hira, A. Sampath Kumar, U. Gupta, P. Pratim Manna, S.P. Singh, Structural characterization and *in vitro* bioactivity assessment of SiO_2–CaO–P_2O_5–K_2O–Al_2O_3 glass as bioactive ceramic material, Ceram. Int. 41 (2015) 11756–11769, https://doi.org/10.1016/j.ceramint.2015.05.143.

[29] C. Wu, W. Fan, M. Gelinsky, Y. Xiao, P. Simon, R. Schulze, T. Doert, Y. Luo, G. Cuniberti, Bioactive SrO-SiO2glass with well-ordered mesopores: characterization, physiochemistry and biological properties, Acta Biomater. 7 (2011) 1797–1806, https://doi.org/10.1016/j.actbio.2010.12.018.

[30] M.S. Bahniuk, H. Pirayesh, H.D. Singh, J.A. Nychka, L.D. Unsworth, Bioactive glass 45S5 powders: effect of synthesis route and resultant surface chemistry and crystallinity on protein adsorption from human plasma, Biointerphases 7 (2012) 1–15, https://doi.org/10.1007/s13758-012-0041-y.

[31] J. Serra, P. González, S. Liste, S. Chiussi, B. León, M. Pérez-Amor, H.O. Ylänen, M. Hupa, Influence of the non-bridging oxygen groups on the bioactivity of silicate glasses, J. Mater. Sci. Mater. Med. (2002) 1221–1225, https://doi.org/10.1023/A:1021174912802.

[32] D. Mondal, S. So-Ra, B.T. Lee, Fabrication and characterization of ZrO_2-CaO-P_2O_5-Na_2O-SiO_2 bioactive glass ceramics, J. Mater. Sci. 48 (2013) 1863–1872, https://doi.org/10.1007/s10853-012-6956-3.

[33] S. Yucel, D. Özçimen, P. Terziőglu, S. Acar, C. Yaman, Preparation of melt derived 45S5 bioactive glass from rice hull ash and its characterization, Adv. Sci. Lett. 19 (2013) 3477–3481, https://doi.org/10.1166/asl.2013.5228.

[34] U. Kalapathy, A. Proctor, J. Shultz, A simple method for production of pure silica from rice hull ash, Bioresour. Technol. 73 (2000) 257–262, https://doi.org/10.1016/S0960-8524(99)00127-3.

[35] L.L. Hench, J. Wilson, An Introduction to Bioceramics, WORLD SCIENTIFIC, 1993, https://doi.org/10.1142/2028.

[36] M.M. Babu, P.S. Prasad, P. Venkateswara Rao, N.P. Govindan, R.K. Singh, H.W. Kim, N. Veeraiah, Titanium incorporated Zinc-Phosphate bioactive glasses for bone tissue repair and regeneration: impact of Ti4 + on physico-mechanical and *in vitro* bioactivity, Ceram. Int. 45 (2019) 23715–23727, https://doi.org/10.1016/j.ceramint.2019.08.087.

[37] V. Cannillo, F. Chiellini, P. Fabbri, A. Sola, Production of Bioglass® 45S5 - polycaprolactone composite scaffolds via salt-leaching, Compos. Struct. 92 (2010) 1823–1832, https://doi.org/10.1016/j.compstruct.2010.01.017.

[38] G. Goller, H. Demirkiran, F.N. Oktar, E. Demirkesen, Processing and characterization of bioglass reinforced hydroxyapatite composites, Ceram. Int. 29 (2003) 721–724, https://doi.org/10.1016/S0272-8842(02)00223-7.

[39] Z. Neščáková, K. Zheng, L. Liverani, Q. Nawaz, D. Galusková, H. Kaňková, M. Michálek, D. Galusek, A.R. Boccaccini, Multifunctional zinc ion doped sol – gel derived mesoporous bioactive glass nanoparticles for biomedical applications, Bioact. Mater. 4 (2019) 312–321, https://doi.org/10.1016/j.bioactmat.2019.10.002.

[40] S.K. Arepalli, H. Tripathi, P.P. Manna, P. Pankaj, S. Krishnamurthy, S.C.U. Patne, R. Pyare, S.P. Singh, Preparation and in vitro investigation on bioactivity of magnesia-contained bioactive glasses, J. Australas. Ceram. Soc. 55 (2019) 145–155, https://doi.org/10.1007/s41779-018-0220-5.

[41] M. Ershad, V.K. Vyas, S. Prasad, A. Ali, R. Pyare, Effect of Sm2O3 substitution on mechanical and biological properties of 45S5 bioactive glass, J. Australas. Ceram. Soc. 54 (2018) 621–630, https://doi.org/10.1007/s41779-018-0190-7.

[42] M. Mozafari, F. Moztarzadeh, M. Tahriri, Investigation of the physico-chemical reactivity of a mesoporous bioactive SiO_2-CaO-P_2O_5 glass in simulated body fluid, J. Non-Cryst. Solids 356 (2010) 1470–1478, https://doi.org/10.1016/j.jnoncrysol.2010.04.040.

[43] A.R. Boccaccini, Q. Chen, L. Lefebvre, L. Gremillard, J. Chevalier, Sintering, crystallisation and biodegradation behaviour of Bioglass®-derived glass-ceramics, Faraday Discuss 136 (2007) 27–44, https://doi.org/10.1039/b616539g.

[44] C. Wu, Y. Xiao, Article commentary: evaluation of the *in vitro* bioactivity of bioceramics , bone tissue regen, Insights 2 (2009), https://doi.org/10.4137/btri.s3188

BTRI.S3188.
[45] Z. Goudarzi, N. Parvin, F. Sharifianjazi, Formation of hydroxyapatite on surface of SiO_2– P_2O_5–CaO–SrO–ZnO bioactive glass synthesized through sol-gel route, Ceram. Int. 45 (2019) 19323–19330, https://doi.org/10.1016/j.ceramint.2019.06.183.
[46] B. Naveen Kumar Reddy, P. Kiran, Effect of silver oxide on hydroxy carbonated apatite formation for simulated body fluid soaked calcium phospho silicate system, Mater. Today Proc. (2019), https://doi.org/10.1016/j.matpr.2019.10.097.
[47] H.S. Mansur, H.S. Costa, Nanostructured poly(vinyl alcohol)/bioactive glass and poly(vinyl alcohol)/chitosan/bioactive glass hybrid scaffolds for biomedical applications, Chem. Eng. J. 137 (2008) 72–83, https://doi.org/10.1016/j.cej.2007.09.036.
[48] S. Hesaraki, M. Alizadeh, H. Nazarian, D. Sharifi, Physico-chemical and *in vitro* biological evaluation of strontium/calcium silicophosphate glass, J. Mater. Sci. Mater. Med. 21 (2010) 695–705, https://doi.org/10.1007/s10856-009-3920-0.
[49] V. Anand, K.J. Singh, K. Kaur, H. Kaur, D.S. Arora, B2O3–MgO–SiO_2–Na_2O–CaO–P_2O_5–ZnO bioactive system for bone regeneration applications, Ceram. Int. 42 (2016) 3638–3651, https://doi.org/10.1016/j.ceramint.2015.11.029.
[50] M.G. Cerruti, D. Greenspan, K. Powers, An analytical model for the dissolution of different particle size samples of Bioglass® in TRIS-buffered solution, Biomaterials 26 (2005) 4903–4911, https://doi.org/10.1016/j.biomaterials.2005.01.013.